Thermochemistry of strontium incorporation in aragonite from atomistic simulations

4 AUTHORS, INCLUDING:

Ricardo Grau-Crespo
University of Reading
72 PUBLICATIONS **770** CITATIONS

SEE PROFILE

A. Rabdel Ruiz-Salvador
Universidad Pablo de Olavide
52 PUBLICATIONS **707** CITATIONS

SEE PROFILE

Nora H. de Leeuw
Cardiff University
240 PUBLICATIONS **4,417** CITATIONS

SEE PROFILE

Volume 74, Number 4
February 15, 2010

Articles

Thermochemistry of strontium incorporation in aragonite from atomistic simulations

Sergio E. Ruiz-Hernandez [a,b,c], Ricardo Grau-Crespo [b,*], A. Rabdel Ruiz-Salvador [c,*], Nora H. De Leeuw [b]

[a] *National Aquarium of Cuba, Ave. 3ra, Esquina 62, Miramar, Havana, Cuba*
[b] *Department of Chemistry, University College London, 20 Gordon Street, London WC1H 0AJ, UK*
[c] *Zeolites Engineering Laboratory, Institute of Materials Research and Engineering (IMRE), University of Havana, Havana 10400, Cuba*

Abstract

We have investigated the thermodynamics of mixing between aragonite (orthorhombic $CaCO_3$) and strontianite ($SrCO_3$). In agreement with experiment, our simulations predict that there is a miscibility gap between the two solids at ambient conditions. All $Sr_xCa_{1-x}CO_3$ solids with compositions $0.12 < x < 0.87$ are metastable with respect to separation into a Ca-rich and a Sr-rich phase. The concentration of Sr in coral aragonites ($x \sim 0.01$) lies in the miscibility region of the phase diagram, and therefore formation of separated Sr-rich phases in coral aragonites is not thermodynamically favorable. The miscibility gap disappears at around 380 K. The enthalpy of mixing, which is positive and nearly symmetric with respect to $x = 0.5$, is the dominant contribution to the excess free energy, while the vibrational and configurational entropic contributions are small and of opposite sign. We provide a detailed comparison of our simulation results with available experimental data.
© 2009 Elsevier Ltd. All rights reserved.

1. INTRODUCTION

Aragonite is one of the three polymorphs of anhydrous calcium carbonate ($CaCO_3$), which also include calcite and vaterite. Although calcite is the most stable $CaCO_3$ phase at Earth surface conditions, aragonite is still a very common mineral, of both geological and biological origin. In particular, aragonite is the major constituent of coral reefs, shells, pearls and other biominerals, where it grows preferentially at ambient conditions due to the effect of organic templates (Morse and Mackenzie, 1990). Strontium is always present in coral aragonites, and it is well established that the precise Sr/Ca ratio in the coral skeleton (typically around 9×10^{-3}) exhibits an inverse correlation with the seawater temperature during its biomineralization (Weber, 1973; Smith et al., 1979; De Villiers et al., 1994). This correlation has led to the use of Sr/Ca ratios in scleractinian corals in the estimation of past sea surface temperatures for the reconstruction of global climate change (Beck et al., 1992; Guilderson et al., 1994; McCulloch et al., 1994), but the mechanism of Sr incorporation in aragonite and the cause of the temperature dependence are not yet clear, which has led to doubts of the validity of these estimations (Schrag and Linsley, 2002). Beck et al. (1992) have claimed that the coral Sr/Ca ratio is controlled by the Sr/Ca ratio in seawater (which is practically constant at $\sim 8.6 \times 10^{-3}$) and the Sr/Ca distribution coefficient between aragonite and seawater, which depends on temperature. However, recent work by other authors suggest that the Sr incorporation in aragonite involves more complicated biological mechanisms and therefore is not thermodynamically controlled (Levi et al., 1998).

It was proposed early on that Sr occupies bulk lattice positions (substituting Ca) in the aragonite structure (Amiel et al., 1973). However, X-ray absorption spectroscopy studies by

* Corresponding authors. Tel.: +44 20 7679 1083; fax: +44 20 7679 7463 (R. Grau-Crespo).

E-mail addresses: r.grau-crespo@ucl.ac.uk (R. Grau-Crespo), rabdel@fisica.uh.cu (A.R. Ruiz-Salvador).

Greegor et al. (1997) suggested that in scleractinian corals with overall Sr/Ca molar ratios of about 8.6×10^{-3}, only 60% of the Sr was in the aragonite lattice, while the remaining 40% resided in strontianite ($SrCO_3$), which is iso-structural to aragonite. As the authors pointed out, the Sr concentration in the aragonite phase is then within the limits of thermodynamic stability of the $Sr_xCa_{1-x}CO_3$ solid solution with respect to phase separation, as determined by Plummer and Busenberg (1987), who found a miscibility gap in the range $5.8 \times 10^{-3} < x < 0.875$ at room temperature. The presence of strontianite in the coral skeleton has been disputed by other authors, who have found no evidence of a Sr-rich phase in a wide range of corals, using similar characterization techniques (Finch and Allison, 2003; Finch et al., 2003; Allison et al., 2005). The implication of the latter group of studies, if the miscibility gap determined by Plummer and Busenberg (1987) is accepted, is that coral aragonite has a metastable Sr/Ca ratio, which would be kept for millions of years because of the slow cation diffusion kinetics at ambient conditions. This is indeed a plausible scenario. However, as discussed below, thermochemical studies by other authors indicate that the limit of stable substitutional Sr in aragonite at ambient conditions is much higher, around 0.10–0.14, which would mean that Sr content in coral aragonite is thermodynamically stable with respect to phase separation.

In this work we investigate the thermodynamics of Sr incorporation in aragonite (structure shown in Fig. 1) using atomistic simulation techniques in combination with statistical mechanics. Our approach is fully predictive, in that no use of experimental information has been made (except, of

course, in the original derivation of the interatomic force field). Our main aim is to produce a theoretical estimate of the maximum Sr content that is thermodynamically stable in aragonite. Our investigation will also allow us to reach a microscopic-level understanding of the factors controlling the stability of Sr impurities in the aragonite structure.

2. METHODOLOGY

2.1. Evaluation of energies and free energies and geometry predictions

Our energy calculations are based on the Born model of solids (Born and Huang, 1954) which assumes that the ions in the crystal interact via long-range electrostatic forces and short-range forces, including both the repulsions and the van der Waals attractions between neighboring electron charge clouds. The electronic polarizability of the ions is included via the shell model of Dick and Overhauser (1958), in which each polarizable ion, in our case the oxygen ion, is represented by a core and a massless shell, connected by a spring. The spring constant and the charges of the core and shell determine the polarizability of the modeled ion. The functional forms of the interatomic potentials are discussed elsewhere (e.g. Catlow, 1997). The $CaCO_3$ potential parameters employed in this study were originally derived by Pavese et al. (1992), and were slightly modified later for a better description of the covalent bonding in the carbonate ion (Pavese et al., 1996). It was found that they correctly describe the vibrational and thermal properties of both calcite and aragonite (Pavese et al., 1992, 1996; Catti et al., 1993). A compatible $SrCO_3$ potential was derived by De Leeuw et al. (2002) and was used by these authors in the simulation of the incorporation of Sr impurities in calcite surfaces and bulk (see also De Leeuw, 2002). A summary of all the potential parameters is given in Table 1.

The lattice energies, as defined by the interatomic potentials, were calculated with the GULP code (Gale, 1997, 2005; Gale and Rohl, 2003). In order to make geometry predictions, the lattice energies are minimized with respect to the structural parameters, until the forces acting on the ions are all less than 0.001 eV Å^{-1}. All structures reported are the result of constant pressure energy minimizations, where not only the ionic positions but also the cell parameters are allowed to vary to find the energy minimum. The external pressure was set to zero in all calculations. Table 2 shows a comparison of the calculated and experimental cell parameters for pure aragonite and strontianite. The theoretical predictions are within 3% of the experimental values.

Finally, since we aim to simulate the behavior of the material at finite temperatures, vibrational contributions to the free energy were also obtained for each relaxed structure, by calculating the phonon frequencies in a mesh of points in the Brillouin zone (Dove, 1993), as implemented in the GULP code. The convergence of the free energy contributions with respect to the reciprocal space partition was carefully checked for pure aragonite and strontianite. We found that in both cases a $5 \times 5 \times 5$ mesh of k-points is enough to achieve convergence within 0.2 kJ/mol in the unit
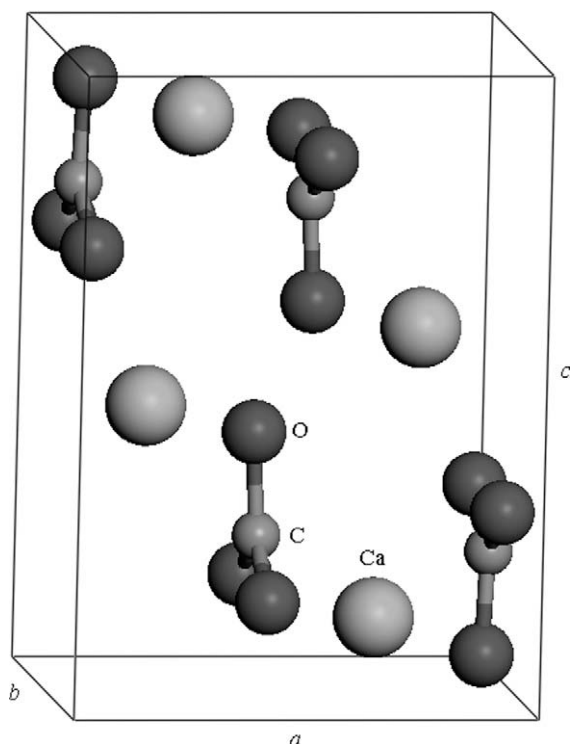

Fig. 1. The orthorhombic unit cell of aragonite (space group Pnma).

Table 1
Interatomic potential parameters used in this work. A cutoff distance of 20 Å was applied to all the short-range potentials.

Species	Charge (e)		Spring constant (eV Å^{-2})
	Core	Shell	
Ca, Sr	+2.0	—	—
C	+1.135	—	—
O	+0.587	−1.632	507.4
Morse potential	D (eV)	α (Å^{-1})	r_0 (Å)
C–O$_{shell}$	4.71	3.8	1.18
Buckingham potential	A (eV)	ρ (Å)	C (eV Å^6)
Ca–O$_{shell}$	1550.0	0.29700	0.0
Sr–O$_{shell}$	1153.5	0.32200	0.0
O$_{shell}$–O$_{shell}$	16372.0	0.21300	3.47
Three-body potential		k (eV rad^{-2})	Θ_0
O$_{core}$–C–O$_{core}$		1.690	120.0
Four-body potential	n	k (eV rad^{-2})	Θ_0
C–O$_{core}$–O$_{core}$–O$_{core}$	2.0	0.1129	180.0

Table 2
Experimental (De Villiers, 1971) and theoretical cell parameters of orthorhombic aragonite (CaCO$_3$) and strontianite (SrCO$_3$). The angles $\alpha = \beta = \gamma = 90°$ are correctly reproduced by the calculations.

Mineral	Space group	a/Å		b/Å		c/Å	
		Exp.	Theo.	Exp.	Theo.	Exp.	Theo.
Aragonite	Pnma (62)	5.740	5.791	4.961	4.831	7.967	7.836
Strontianite	Pnma (62)	5.997	6.100	5.090	4.946	8.358	8.110

cells, and we therefore keep the same or higher k-point densities in all our calculations (larger supercells require fewer k-points to achieve the same mesh density in the reciprocal space). In principle, it is also possible to account for thermal effects on the structure of each configuration by performing a free energy minimization at each geometry and temperature, using the quasi-harmonic approximation (e.g. Taylor et al., 1997; Gale, 1998; Grau-Crespo et al., 2002). However, considering the large number of configurations treated here and the high computational cost of free energy minimizations, we have optimized the structures only with respect to the lattice energy. The vibrational free energies were then obtained in the harmonic approximation at the energy-minimized structures, without further optimization. Although this approach does not account for structural effects of thermal origin, like thermal expansion, it can be expected to be adequate for the investigation of the vibrational energetic contributions to the mixing thermodynamics.

2.2. Configurational statistics

The distribution of Sr in the aragonite lattice was investigated utilizing the SOD (Site Occupancy Disorder) code (Grau-Crespo et al., 2007), which generates the complete configurational space for each composition in a supercell of the structure, before extracting the subspace of symmetrically inequivalent configurations, which are the ones calculated in GULP. The criterion for the equivalence of two configurations is the existence of an isometric transfor-

mation that converts one configuration into the other, where the transformations considered are simply the symmetry operators of the *parent* structure (the structure from which all configurations are derived via site substitutions). Once the configurational spectrum is obtained, it is possible to derive configurational entropies and free energies. The methodology is based on the assumption that the extent of occurrence of one particular configuration in the disordered solid can be described by a Boltzmann-like probability which can be calculated from the vibrational free energy G_m of the configuration, and its degeneracy Ω_m (the number of times that the configuration is repeated in the complete configurational space):

$$P_m = \frac{1}{Z}\Omega_m \exp(-G_m/k_B T) = \frac{1}{Z}\exp(-G_m^*/k_B T) \qquad (1)$$

where $m = 1, \ldots, M$ (M is the number of inequivalent configurations), k_B is Boltzmann's constant (it is formally equivalent to use the gas constant R instead, but we follow here the usual notation in statistical mechanics),

$$Z = \sum_{m=1}^{M} \exp(-G_m^*/k_B T) \qquad (2)$$

is the partition function, and we have introduced the reduced free energy:

$$G_m^* = G_m - TS_m^* \qquad (3)$$

which contains contributions from both the vibrational entropy and from the degeneracy entropy of the configuration:

$$S_m^* = k_B T \ln \Omega_m \quad (4)$$

The configurational free energy G of the disordered solid can be obtained directly from the partition function:

$$G = -k_B T \ln Z \quad (5)$$

and any average observable, including the enthalpy H of the solution, can be estimated using configurational averaging:

$$H = \sum_{m=1}^{M} P_m H_m \quad (6)$$

In our case, since no external pressure is considered, the enthalpy is simply the energy of each configuration. The configurational entropy at any temperature and composition can then be obtained as:

$$S = \frac{H - G}{T} = -k_B \sum_{m=1}^{M} P_m \ln P_m + \sum_{m=1}^{M} P_m S_m^* \quad (7)$$

We can therefore obtain the free energy of a solid solution, including energetic, vibrational and configurational effects, by obtaining first the configurational spectrum of energies in the supercell of the structure. The total number of configurations, and the number of inequivalent ones for each composition in the $2 \times 2 \times 1$ and the $2 \times 2 \times 2$ supercells are given in Table 3. The number of configurations scales very quickly with the size of the supercell. We will show below that our results are well converged with respect to the supercell size, as very similar results are obtained with both supercells. This type of methodology, with some variations, has been applied successfully in the simulation of the thermodynamics of mineral solid solutions (Becker et al., 2000; Lavrentiev et al., 2003; Todorov et al., 2004) and the investigation of cation distributions in oxide materials (Grau-Crespo et al., 2003, 2004; Benny et al., 2009).

Table 3
Total number of configurations (N) and number of symmetrically inequivalent configurations (M) for each composition $Sr_xCa_{1-x}CO_3$ in the $2 \times 2 \times 1$ $((A,B)_{16}(CO_3)_{16})$ and $2 \times 2 \times 2$ $((A,B)_{32}(CO_3)_{32})$ supercells. A and B stand for either Ca or Sr.

Cell composition	x or $1-x$	N	M
$A_{16}(CO_3)_{16}$	0	1	1
$A_{15}B(CO_3)_{16}$	0.063	16	1
$A_{14}B_2(CO_3)_{16}$	0.125	120	9
$A_{13}B_3(CO_3)_{16}$	0.188	560	23
$A_{12}B_4(CO_3)_{16}$	0.250	1820	82
$A_{11}B_5(CO_3)_{16}$	0.313	4368	157
$A_{10}B_6(CO_3)_{16}$	0.375	8008	303
$A_9B_7(CO_3)_{16}$	0.438	11,440	395
$A_8B_8(CO_3)_{16}$	0.500	12,870	474
$A_{32}(CO_3)_{32}$	0	1	1
$A_{31}B(CO_3)_{32}$	0.031	32	1
$A_{30}B_2(CO_3)_{32}$	0.063	496	17
$A_{29}B_3(CO_3)_{32}$	0.094	4960	99
$A_{28}B_4(CO_3)_{32}$	0.125	35,960	694

2.3. Evaluation of the mixing thermodynamic potentials

Having obtained the enthalpy and free energy of the solid solution, it is useful to evaluate the enthalpy of mixing:

$$\Delta H_{mix} = H[Sr_xCa_{1-x}CO_3] - (1-x)H[CaCO_3]$$
$$- xH[SrCO_3] \quad (8)$$

which can be compared with experimental calorimetric determinations, and the free energy of mixing:

$$\Delta G_{mix} = G[Sr_xCa_{1-x}CO_3] - (1-x)G[CaCO_3]$$
$$- xG[SrCO_3] \quad (9)$$

which can also be found experimentally from equilibrium composition measurements, e.g. using electrochemical cells. In Eqs. (8) and (9), all the energies are given per formula unit. $\Delta G_{mix}(x)$ quantifies the stability of the mixed solid with respect to the pure end-members, aragonite ($CaCO_3$) and strontianite ($SrCO_3$). It is common to report the excess free energies of the solution, defined as:

$$G^E(x) = \Delta G_{mix} - \Delta G_{mix}^{ideal} \quad (10)$$

where

$$\Delta G_{mix}^{ideal}(x) = k_B T[x \ln x + (1-x)\ln(1-x)] \quad (11)$$

is the free energy of mixing in an ideal solid solution, where the only contribution comes from the ideal entropy corresponding to a fully disordered solid. The excess free energy G^E therefore contains all the non-ideal contributions to the mixing free energy: an enthalpy part (ΔH_{mix}), and an entropy part, which contains both the deviation of the configurational entropy from ideality and a contribution from the vibrational entropy of mixing. Our simulation method allows us to separate all these different contributions.

Excess free energies from experiment are commonly fitted to a polynomial of the mole fraction x in the form given by Guggenheim (1937):

$$G^E = x(1-x)[A_0 + A_1(2x-1) + \cdots] \quad (12)$$

which can be expanded to higher orders of $2x - 1$. Different types of solid solution behavior can be expressed in terms of Eq. (12). Ideal solutions, for example, correspond to the case $A_0 = A_1 = A_2 = \cdots = 0$, while the case where $A_0 \neq 0$, $A_2 = A_3 = \cdots = 0$ is the so-called regular solution (strictly regular if A_0 does not depend on temperature, e.g. Plummer and Busenberg, 1987; Prieto et al., 2000). We will fit our calculated G^E values to this type of polynomials in order to compare with experimental information. The fitted function will also allow us to calculate numerically the miscibility gap in the solid solution, which is marked by two minima of $\Delta G_{mix}(x)$.

3. RESULTS AND DISCUSSION

The equilibrium geometries and energies of the Sr-substituted configurations were calculated both without and including vibrational effects, in the $2 \times 2 \times 1$ (16 cation sites) and $2 \times 2 \times 2$ (32 cation sites) supercells of the aragonite structure. The unit cell of aragonite contains four cation sites (Fig. 1). A list of calculated configurations is

presented in Table 3, where x determines the composition of the solid solution $Sr_xCa_{1-x}CO_3$. For the $2 \times 2 \times 2$ supercell, other concentrations than those shown were not considered, due to the prohibitive computational cost. It will be shown below that the use of a smaller supercell does not change the results significantly.

Because aragonite and strontianite are iso-structural, the introduction of impurity cations in either material does not affect the structure significantly beyond small local relaxations. We find that the lowest-energy Sr-doped aragonite structures are those with shorter Sr–Sr distances, although the calculated interaction between impurities is small. We therefore do not expect that Sr impurities will form clusters, because at the low concentrations of interest here the number of configurations with more homogeneous Sr distributions is much larger than those exhibiting impurity aggregation, and this entropic effect is much stronger than the weak stabilization provided by the interaction between impurities. For example, the spectrum of configurations corresponding to the strontium concentration $x = 0.125$, obtained with the $2 \times 2 \times 2$ supercell ($Sr_4Ca_{28}(CO_3)_{32}$) at 300 K is shown in Fig. 2, where the zero-level is defined as the reduced free energy of the most probable configuration. Nearly half of the configurations lie within $k_BT = 2.49$ kJ/mol, indicating that a great deal of disorder
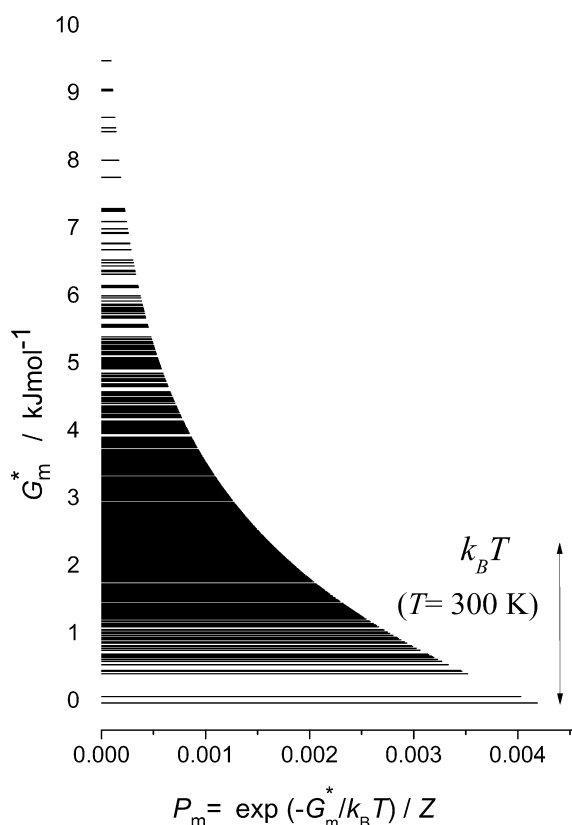
should be expected in the Sr distribution. However, there is some deviation from a uniform probability distribution, which will translate into a reduced configurational entropy compared with an ideal solid solution.

Fig. 3(a) shows the enthalpies of mixing as a function of Sr concentration, calculated using Eqs. (6) and (8) for both the $2 \times 2 \times 1$ and the $2 \times 2 \times 2$ supercells. The formation of the solid solution from pure aragonite and strontianite is endothermic in the whole range of compositions, as expected from the difference in ionic radii (Shannon, 1976) between Ca^{2+} (1.18 Å) and Sr^{2+} (1.31 Å) in ninefold coordination. Our theoretical values are not far from the calorimetric measurements by Casey et al. (1996a), especially when considering the small values involved and the wide error bars and dispersion of the experimental points. These authors fitted their data to a symmetric curve in the form:

$$\Delta H_{mix} = Wx(1 - x) \tag{13}$$

and found $W = 13.5$ kJ/mol. We will argue below that this value of W is probably too high, not only in comparison with our calculations but also in the light of experimental determinations of mixing free energies by the same and other authors. Using the same model to fit our data from the $2 \times 2 \times 1$ supercell leads to $W = 5.84$ kJ/mol, although an asymmetric model in the form:

Fig. 2. Configurational spectrum of reduced free energies corresponding to the composition $Sr_{0.125}Ca_{0.875}CO_3$ at 300 K, as calculated in the $2 \times 2 \times 2$ supercell. P_m is the probability of occurrence of the independent configuration, and G_m^* is its reduced free energy.
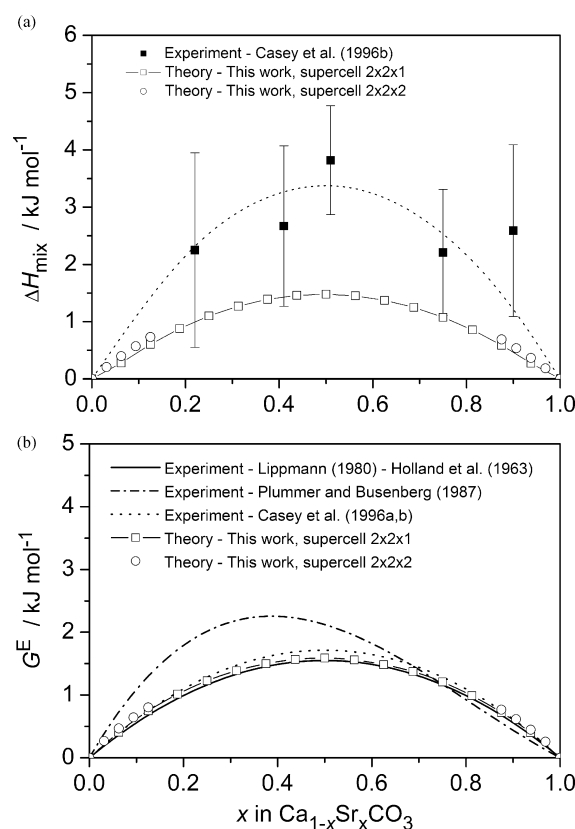

Fig. 3. Aragonite–strontianite mixing under ambient conditions. (a) Calculated and experimental enthalpies of mixing and (b) calculated and experimental excess free energies.

$$\Delta H_{\mathrm{mix}} = x(1-x)[W_0 + W_1(2x-1)] \qquad (14)$$

with $W_0 = 5.84$ kJ/mol and $W_1 = -0.12$ kJ/mol provides a better fit. The slightly asymmetric character of our $\Delta H_{\mathrm{mix}}(x)$ curve, with small and negative W_1, means that the energetic cost of doping aragonite with Sr from strontianite ($W_0 - W_1$) is somewhat higher than the cost of doping strontianite with Ca from aragonite ($W_0 + W_1$). This asymmetry is reasonable, based on the larger ionic radius of Sr compared to Ca, as the incorporation of Sr would lead to a larger elastic strain in the lattice of aragonite than vice versa (McLean, 1957; de Leeuw and Parker, 2000). Fig. 3(a) also shows that using the larger $2 \times 2 \times 2$ supercell does not significantly change our predicted mixing enthalpies. It should be noted here that, since ΔH_{mix} is just one of the contributions to the excess free energy, we make a distinction between W_0 and W_1 in Eq. (14), and the A_0 and A_1 parameters of the Guggenheim expression (Eq. (12)) for the excess free energy. The connection between the two sets of parameters will be discussed below.

The calculated excess free energy at 300 K is shown in Fig. 3(b), together with experimental determinations (fitting curves) by other authors. Our fitting to a Guggenheim polynomial of first order in $2x - 1$ (Eq. (12)) leads to $A_0 = 6.43$ kJ/mol and $A_1 = -0.12$ kJ/mol, which is practically symmetric around $x = 0.5$ (very small A_1 value), in contrast with the strongly asymmetric curve proposed by Plummer and Busenberg (1987) to fit their experimental measurements under ambient conditions. In the picture proposed by these authors, it is much more difficult to dope aragonite with Sr ($A_0 - A_1 = 13$ kJ/mol) than strontianite with Ca ($A_0 + A_1 = 4$ kJ/mol). However, our theoretical results are in very good agreement with experimental data from other authors. Lippmann (1980), for example, treated the data obtained by Holland et al. (1963), and suggested a symmetric model with $A_0 = 6.2$ kJ/mol. Also, some of the same authors who published the calorimetric study (Casey et al., 1996a), reported excess free energy measurements using an electrochemical cell (Casey et al., 1996b), and their results in this case are in very good agreement with our data.

A summary of all experimental and theoretical Guggenheim parameters is given in Table 4. We also report there the values obtained from our simulations at 350 and 400 K. It can be seen that, while A_1 remains constant and small, A_0 increases slightly with temperature up to 6.70 kJ/mol at 400 K. Using a linear interpolation for A_1
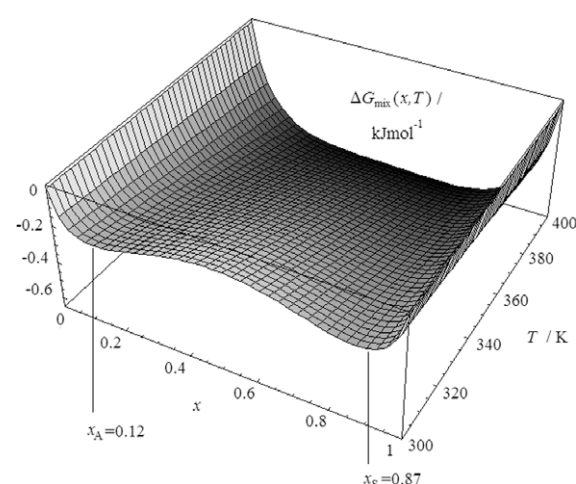

Fig. 4. Theoretical free energy of mixing as a function of temperature and composition x in $Sr_xCa_{1-x}CO_3$. The minima x_A and x_S mark the predicted limits of the thermodynamic miscibility gap between aragonite and strontianite under ambient conditions.

we can obtain free energy of mixing curves at temperatures between 300 and 400 K, as shown in Fig. 4. At ambient temperature, the free energy of mixing has two minima at $x_A = 0.12$ and $x_S = 0.87$, which define a miscibility gap between aragonite and strontianite. Any solid with composition $x_A < x < x_S$ is metastable with respect to a mechanical mixture of phases with composition x_A (Sr-doped aragonite) and x_S (Ca-doped strontianite).

The prediction of a miscibility gap in the aragonite–strontianite system under ambient conditions is in agreement with most experimental studies, and with the absence of intermediate compositions in natural solid solutions (Speer, 1983). While all authors basically agree on the upper limit of the miscibility gap (x_S) being around 0.86–0.90 (our theoretical prediction is 0.87), the lower limit of the miscibility gap is less clear (see Table 4). Plummer and Busenberg (1987) predict a low value of equilibrium Sr content in aragonite ($x_A = 0.0058$) while Lippmann (1980) and Casey et al. (1996b) predict higher values (0.10 and 0.14). We note that the Sr content of the coral skeleton ($x \sim 0.01$) is intermediate between the two sets of results, and therefore discrimination between the two types of behavior is important in order to elucidate the stable or metastable character of Sr incorporation in coral arago-

Table 4
Summary of fitting parameters for the excess free energy $G^E = x(1-x)[A_0 + A_1(2x-1)]$, as obtained experimentally by other authors and theoretically in this work.

T/K	Reference	A_0/kJ mol^{-1}	A_1/kJ mol^{-1}	x_A	x_S
298.15	Experimental—Lippmann (1980) and Holland et al. (1963)	6.2	0	0.14	0.86
	Experimental—Plummer and Busenberg (1987)	8.48	−4.51	0.0058	0.88
	Experimental—Casey et al. (1996a,b)	6.86	0	0.10	0.90
300	Theory—this work	6.43	−0.12	0.12	0.87
		(6.93)[a]	(−0.12)[a]	(0.09)[a]	(0.90)[a]
349.15	Experimental—Plummer and Busenberg (1987)	7.71	−3.36	0.031	0.83
350	Theory—this work	6.57	−0.12	0.22	0.78
400	Theory—this work	6.70	−0.12	—	—

[a] Values in parenthesis are those calculated without including vibrational contributions.

nites. Our theoretical result (0.12) supports the second set of values, and therefore suggests that Sr is stable in corals with respect to phase separation. Fig. 4 also shows that the predicted miscibility gap becomes narrower with increasing temperature, and disappears completely at around 380 K.

Let us now discuss the different contributions to the excess free energy. It is clear that the small (and temperature-independent) effect introduced by the parameter A_1 in the excess free energy arises from the asymmetry of the enthalpy of mixing ($A_1 = W_1$). Therefore we will focus on the different contributions to A_0. By fitting the excess free energies obtained with and without vibrational contributions, we are able to do an approximate decomposition:

$$A_0 = W_0 + \Delta A_0^{conf} + \Delta A_0^{vib} \qquad (15)$$

where $W_0 = 5.84$ kJ/mol is the enthalpic contribution, which remains practically constant in the temperature interval of interest here, while ΔA_0^{conf} and ΔA_0^{vib} are the configurational and vibrational entropic contributions. At 300 K, $\Delta A_0^{conf} = 1.09$ kJ/mol and $\Delta A_0^{vib} = -0.50$ kJ/mol. The vibrational contribution lowers the free energies of mixing, as can be seen in Fig. 5, and the contribution becomes more negative at higher temperatures. On the other hand, the configurational contribution to the excess free energy is positive because the real configurational entropy is lower than the ideal one corresponding to full disorder, as discussed above. Therefore, since the two entropic contributions are relatively small and of opposite sign, the dominant contribution to the excess free energy becomes the enthalpy of mixing, which accounts for the similarity between the $\Delta H_{mix}(x)$ and the $G^E(x)$ curves in Fig. 3(a) and (b). Thus, the solid solution is nearly regular, because it has very small excess entropy. The total excess entropy should be even lower because the configurational contribution is overestimated here due to the periodicity of the simulation supercell, which imposes some constraints on the level of disorder. The present analysis indicates that the difference between the calorimetric and the free energy data of Casey et al. is unlikely to be accounted for by non-ideal entropic effects. Our theoretical simulations, together with the results published by Lippmann (1980) and Holland et al.
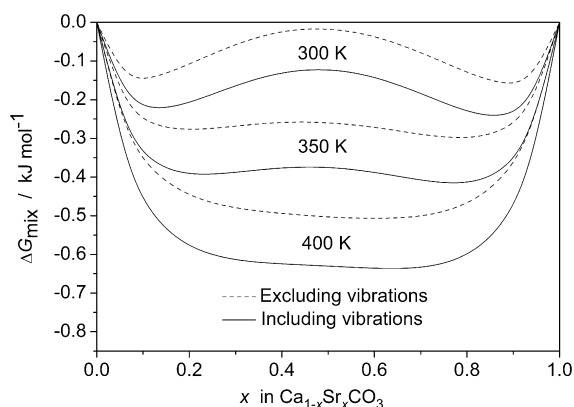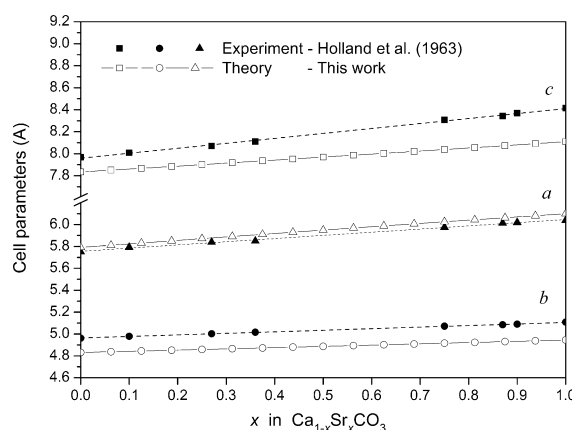

Fig. 6. Variation of the calculated cell parameters for the $Sr_xCa_{1-x}CO_3$ solid solution with composition, in comparison with experiment.

(1963), add support to their free energy determinations, rather than to their calorimetric measurements (Fig. 6).

We have also calculated the cell parameters in the aragonite–strontianite as a function of composition, assuming a high temperature (400 K) at which all compositions are stable. At each composition, the cell parameters are obtained as configurational averages:

$$a = \sum_{m=1}^{M} P_m a_m; \quad b = \sum_{m=1}^{M} P_m b_m; \quad c = \sum_{m=1}^{M} P_m c_m \qquad (16)$$

where a_m, b_m and c_m are the cell parameters of the mth independent configuration. Our data do not include thermal expansion effects as mentioned in Section 2.1. In order to avoid confusion, we note here that the aragonite and strontianite crystallographic structures are sometimes reported in the Pmcn space group (No. 62), for which $a < c < b$ (e.g. Holland et al., 1963), while other authors (e.g. Lucas-Girot et al., 2007) use the Pnma setting of the same space group, for which $b < a < c$. Here we will use the latter setting. Our results show that, as expected from the larger radius of Sr^{2+} compared to Ca^{2+}, all the cell parameters increase with x. Small departures from the linear dependences were reported by Holland et al. (1963), who found that the a dimension lies slightly above and the c dimension slightly below the lines joining the end-members. However, in our calculations all the cell dimensions vary linearly with composition, which is in agreement with more recent X-ray diffraction data by Lucas-Girot et al. (2007).

4. CONCLUSIONS

We have performed an atomistic simulation study of the mixing thermodynamics of aragonite–strontianite solid solutions in the whole range of compositions $Sr_xCa_{1-x}CO_3$. We have shown that the dominant contribution to the excess free energy comes from the enthalpy of mixing, while the vibrational and configurational entropic contributions are small and of opposite sign. These findings, together with the nearly symmetric character of the mixing thermodynamic potentials around $x = 0.5$, mean that the

Fig. 5. Effect of vibrations on the calculated free energies of mixing at 300, 350 and 400 K.

aragonite–strontianite mixing behavior is close to the regular solution model. However, the regular behavior is not strict in that (a) there is a small asymmetric contribution to the excess energy and (b) the A_0 parameter in the Guggenheim expression shows some dependence on temperature.

Our simulations predict that at room temperature and up to ~380 K, there is a miscibility gap of thermodynamic origin between aragonite and strontianite. Under ambient conditions, all $Sr_xCa_{1-x}CO_3$ solids with compositions $0.12 < x < 0.87$ are metastable with respect to separation into a Ca-rich and a Sr-rich phase, which agrees well with the results reported by Casey et al. (1996b) and also by Lippmann (1980) based on measurements by Holland et al. (1963), but is in contrast with the results of Plummer and Busenberg (1987), who suggested a much lower miscibility limit for Sr in aragonite (0.0058). Our results suggest that the concentration of Sr in coral aragonite, which is typically around 0.01, is therefore stable in substitutional positions in the aragonite lattice, and should not experience phase separation into strontianite. We should note that, although Greegor et al. (1997) have suggested that a large fraction of Sr in coral skeletons resides in strontianite, more recent experiments have found no evidence of Sr-rich phases in the coral skeletons (e.g. Allison et al., 2005). The discussion presented here is important for the interpretation of coral Sr paleothermometry, as the presence of Sr in other phases than aragonite would complicate the understanding of the correlation between coral Sr/Ca ratios and sea surface temperatures.

REFERENCES

Allison N., Finch A. A., Newville M. and Sutton S. R. (2005) Strontium in coral aragonite: 3. Sr coordination and geochemistry in relation to skeletal architecture. *Geochim. Cosmochim. Acta* **69**(15), 3801–3811.

Amiel A. J., Friedman G. M. and Miller D. S. (1973) Distribution and nature of incorporation of trace-elements in modern aragonitic corals. *Sedimentology* **20**(1), 47–64.

Beck J. W., Edwards R. L., Ito E., Taylor F. W., Recy J., Rougerie F., Joannot P. and Henin C. (1992) Sea-surface temperature from coral skeletal strontium calcium ratios. *Science* **257**(5070), 644–647.

Becker U., Fernandez-Gonzalez A., Prieto M., Harrison R. and Putnis A. (2000) Direct calculation of thermodynamic properties of the barite/celestite solid solution from molecular principles. *Phys. Chem. Miner.* **27**(4), 291–300.

Benny S., Grau-Crespo R. and De Leeuw N. H. (2009) A theoretical investigation of α-Fe_2O_3–Cr_2O_3 solid solutions. *Phys. Chem. Chem. Phys.* **11**, 808–815.

Born M. and Huang K. (1954) *Dynamical Theory of Crystal Lattices*. Oxford University Press.

Casey W. H., Chai L. A., Navrotsky A. and Rock P. A. (1996a) Thermochemistry of mixing strontianite [$SrCO_3(s)$] and aragonite [$CaCO_3(s)$] to form $Ca_xSr_{1-x}CO_3(s)$ solid solutions. *Geochim. Cosmochim. Acta* **60**(6), 933–940.

Casey W. H., Rock P. A., Chung J. B., Walling E. M. and McBeath M. K. (1996b) Gibbs energies of formation of metal carbonate solid solutions: 2. The $Ca_xSr_{1-x}CO_3(s)$ system at 298 K and 1 bar. *Am. J. Sci.* **296**(1), 1–22.

Catlow C. R. A. (1997) *Computer Modelling in Inorganic Crystallography*. Academic Press.

Catti M., Pavese A. and Price G. D. (1993) Thermodynamic properties of $CaCO_3$ calcite and aragonite—a quasi-harmonic calculation. *Phys. Chem. Miner.* **19**(7), 472–479.

De Leeuw N. H. (2002) Molecular dynamics simulations of the growth inhibiting effect of Fe2+, Mg2+, Cd2+, and Sr2+ on calcite crystal growth. *J. Phys. Chem. B* **106**(20), 5241–5249.

De Leeuw N. H. and Parker S. C. (2000) Modeling absorption and segregation of magnesium and cadmium ions to calcite surfaces: Introducing MgCO3 and CdCO3 potential models. *J. Chem. Phys.* **112**(9), 4326–4333.

De Leeuw N. H., Harding J. H. and Parker S. C. (2002) Molecular dynamics simulations of the incorporation of Mg^{2+}, Cd^{2+} and Sr^{2+} at calcite growth steps: introduction of a $SrCO_3$ potential model. *Mol. Simul.* **28**(6–7), 573–589.

De Villiers J. P. R. (1971) Crystal structures of aragonite, strontianite and witherite. *Am. Mineral.* **56**(5–6), 758–767.

De Villiers S., Shen G. T. and Nelson B. K. (1994) The Sr/Ca-temperature relationship in coralline aragonite—influence of variability in (Sr/Ca) seawater and skeletal growth-parameters. *Geochim. Cosmochim. Acta* **58**(1), 197–208.

Dick B. G. and Overhauser A. W. (1958) Theory of the dielectric constant of alkali halide crystals. *Phys. Rev.* **112**, 90–103.

Dove M. T. (1993) *Introduction to Lattice Dynamics*. Cambridge University Press.

Finch A. A. and Allison N. (2003) Strontium in coral aragonite: 2. Sr coordination and the long-term stability of coral environmental records. *Geochim. Cosmochim. Acta* **67**(23), 4519–4527.

Finch A. A., Allison N., Sutton S. R. and Newville M. (2003) Strontium in coral aragonite: 1. Characterization of Sr coordination by extended absorption X-ray fine structure. *Geochim. Cosmochim. Acta* **67**(6), 1189–1194.

Gale J. D. (1997) GULP: a computer program for the symmetry-adapted simulation of solids. *J. Chem. Soc.: Faraday Trans.* **93**(4), 629–637.

Gale J. D. (1998) Analytical free energy minimization of silica polymorphs. *J. Phys. Chem. B* **102**, 5423–5431.

Gale J. D. (2005) GULP: capabilities and prospects. *Z. Kristallogr.* **220**, 552–554.

Gale J. D. and Rohl A. L. (2003) The general utility lattice program (GULP). *Mol. Simul.* **29**(5), 291–341.

Grau-Crespo R., Acuay E. and Ruiz-Salvador R. R. (2002) A free energy minimisation study of the monoclinic–orthorhombic transition in MFI zeolite. *Chem. Commun.* **21**, 2544–2545.

Grau-Crespo R., De Leeuw N. H. and Catlow C. R. A. (2003) Cation distribution and magnetic ordering in $FeSbO_4$. *J. Mater. Chem.* **13**(12), 2848–2850.

Grau-Crespo R., De Leeuw N. H. and Catlow C. R. A. (2004) Distribution of cations in $FeSbO_4$: a computer modeling study. *Chem. Mater.* **16**(10), 1954–1960.

Grau-Crespo R., Hamad S., Catlow C. R. A. and De Leeuw N. H. (2007) Symmetry-adapted configurational modelling of fractional site occupancy in solids. *J. Phys.: Condens. Mat.* **19**, 256201.

Greegor R. B., Pingitore N. E. and Lytle F. W. (1997) Strontianite in coral skeletal aragonite. *Science* **275**(5305), 1452–1454.

Guggenheim E. A. (1937) The theoretical basis of Raoult's law. *Trans. Faraday Soc.* **33**, 151–159.

Guilderson T. P., Fairbanks R. G. and Rubenstone J. L. (1994) Tropical temperature variations since 20,000 years ago—modulating interhemispheric climate change. *Science* **263**(5147), 663–665.

Holland H. D., Borcsik M., Munoz J. and Oxburgh U. M. (1963) The coprecipitation of Sr^{+2} with aragonite and of Ca^{+2} with strontianite between 90 °C and 100 °C. *Geochim. Cosmochim. Acta* **27**, 957–964.

Lavrentiev M. Y., Allan N. L. and Purton J. A. (2003) Beyond the point defect limit: solid solutions, phase diagrams and trace-element partitioning. *Phys. Chem. Chem. Phys.* **5**(11), 2190–2196.

Levi Y., Albeck S., Brack A., Weiner S. and Addadi L. (1998) Control over aragonite crystal nucleation and growth: an in vitro study of biomineralization. *Chemistry* **4**(3), 389–396.

Lippmann F. (1980) Phase diagrams depicting aqueous solubility of binary mineral systems. *Neues Jahrb. Mineral. Abh.* **139**(139), 1–25.

Lucas-Girot A., Hernandez O. and Oudadesse H. (2007) Re-examination of the structural properties of solid solutions $Sr_xCa_{1-x}CO_3$. *Mater. Res. Bull.* **42**(6), 1061–1068.

McCulloch M. T., Gagan M. K., Mortimer G. E., Chivas A. R. and Isdale P. J. (1994) A high-resolution Sr/Ca and Delta-O-18 coral record from the Great–Barrier–Reef, Australia, and the 1982–1983 El-Nino. *Geochim. Cosmochim. Acta* **58**(12), 2747–2754.

McLean D. (1957) *Grain boundaries in metals*. Clarendon, Oxford.

Morse J. W. and Mackenzie F. T. (1990) *Geochemistry of Sedimentary Carbonates*. Elsevier.

Pavese A., Catti M., Price G. D. and Jackson R. A. (1992) Interatomic potentials for $CaCO_3$ polymorphs (calcite and aragonite), fitted to elastic and vibrational data. *Phys. Chem. Miner.* **19**(2), 80–87.

Pavese A., Catti M., Parker S. C. and Wall A. (1996) Modelling of the thermal dependence of structural and elastic properties of calcite, $CaCO_3$. *Phys. Chem. Miner.* **23**(2), 89–93.

Plummer L. N. and Busenberg E. (1987) Thermodynamics of aragonite–strontianite solid-solutions—results from stoichiometric solubility at 25-degrees-C and 76-degrees-C. *Geochim. Cosmochim. Acta* **51**(6), 1393–1411.

Prieto M., Fernandez-Gonzalez A., Becker U. and Putnis A. (2000) Computing Lippmann diagrams from direct calculation of mixing properties of solid solutions: application to the barite–celestite system. *Aquat. Geochem.* **6**(2), 133–146.

Schrag D. P. and Linsley B. K. (2002) Paleoclimate: corals, chemistry, and climate. *Science* **296**(5566), 277–278.

Shannon R. D. (1976) Revised effective ionic radii and systematic studies of interatomic distances in halides and chalcogenides. *Acta Crystallogr. A* **32**, 751–767.

Smith S. V., Buddemeier R. W., Redalje R. C. and Houck J. E. (1979) Strontium–calcium thermometry in coral skeletons. *Science* **204**(4391), 404–407.

Speer, J.A. (1983) Crystal chemistry and phase relations of orthorhombic carbonates. In *Carbonates: Mineralogy and Chemistry*, vol. 11 (ed. R. J. Reeder). Mineral. Soc. Am., Rev. Mineral., pp. 145–190.

Taylor M. B., Barrera G. D., Allan N. L. and Barron T. H. K. (1997) Free-energy derivatives and structure optimization within quasiharmonic lattice dynamics. *Phys. Rev. B* **56**(22), 14380–14390.

Todorov I. T., Allan N. L., Lavrentiev M. Y., Freeman C. L., Mohn C. E. and Purton J. A. (2004) Simulation of mineral solid solutions at zero and high pressure using lattice statics, lattice dynamics and Monte Carlo methods. *J. Phys.: Condens. Mat.* **16**(27), S2751–S2770.

Weber J. N. (1973) Incorporation of strontium into reef coral skeletal carbonate. *Geochim. Cosmochim. Acta* **37**(9), 2173–2190.

Associate editor: Dimitri A. Sverjensky